Check for updates

# Endophytes *Bacillus amyloliquefaciens* AW3 (CGMCC1.16683) improves the growth of *Populus davidiana × Populus bolleana* (PdPap) and induces its resistance to wilt disease by *Fusarium oxysporum* Fox68 (CFCC86068)

**Ping Zhang · Haotian Hao · Lihai Wang · Zhihua Liu · Ling Ma**

**Abstract** *Populus davidiana × Populus bolleana* (PdPap) root rot caused by *Fusarium oxysporum* is a major disease in China. Controlling this disease requires extensive use of chemicals. The use of plant endophytes, such as *Bacillus*, may be a suitable alternative to chemical agents. In this study, we isolated a strain of *Bacillus amyloliquefaciens* (AW3) by thermal stimulation and confrontation method from fleshy tap roots of *Brassica rapa* L. We then determined its inhibitory effect on the growth of *F. oxysporum* (Fox68) and how it induces the disease resistance of PdPap. The confrontation area and roots were visualized using an optical microscope and a scanning electron microscope, respectively, and mycelial cell malformation, swelling, and distortion observed. AW3 and *F. oxysporum* were inoculated in a variety of combinations that reduced the disease level. PdPap defense-related enzymes, such as PAL, PPO, SOD, and CAT, increased significantly. Besides, several genes associated with plant defense and hormonal signal transduction were highly expressed. Under the biological stress of Fox68, AW3 directly acted on the hyphae of Fox68, reducing the infection of PdPap by Fox68 and promoting PdPap growth. AW3 also induced the accumulation of defense-related enzymes/genes that conferred resistance. Therefore, AW3 could serve as a bio-control agent of wilt disease caused by *F. oxysporum* in PdPap.

**Keywords** *Populus davidiana × Populus bolleana* · *Bacillus amyloliquefaciens* · *Fusarium oxysporum* · Biological control · Wilt disease

P. Zhang · L. Wang · Z. Liu (✉) · L. Ma (✉)
State Key Laboratory of Tree Genetics and Breeding (Northeast Forestry University), Harbin 150040, China
e-mail: LZHNEFU@126.com

L. Ma
e-mail: maling63@163.com

P. Zhang
e-mail: ifedu@126.com

L. Wang
e-mail: wanglihai60@yeah.com

H. Hao
INFOSEC Laboratory (Peking University), Beijing 102600, China
e-mail: hht@pku.edu.cn

## Introduction

*Populus davidiana × Populus bolleana* (PdPap) is one of the few tree species with the ability to withstand the harsh conditions of low temperature and drought. It is widely planted in Xinjiang and Northeast China. Although PdPap can tolerate drought, low temperature, and stress, and is resistant to most pests and pathogens, *F. oxysporum* Schltdl often causes

many deaths in the nursery. The aerial part of the diseased plant exhibits withered leaves, and root rot. So far, with fungicides (carbendazim) remains the main method for controlling this disease (Addrah et al., 2019). However, with achievement of sustainable development being the current focus in most parts of the world, reduction of chemical pesticides application adopted. In this essence, biological control is considered the most practical as it is environment friendly (Rabiey et al., 2019). The genus *Fusarium* Link consists of saprophytic soil fungi distributed worldwide. In some specific environments, the strains change from saprophytic to parasites, leading to root rot, plant wilt, and death (Coleman, 2016). *Fusarium* head blight (FHB) caused by *Fusarium* is widespread in major wheat producing areas such as Italy and France, which not only affects wheat production, but also causes many mycotoxins in wheat grains to exceed the standard, posing a serious threat to human and animal health (Gorash et al., 2021). *Bacillus* spp. have been considered the potential biological control agents (BCAs) of PdPap trees against *F. oxysporum*. Nonetheless, few detailed scientific studies have been carried out to establish the efficient protection mechanism of PdPap trees against *F. oxysporum* using the *Bacillus* genus.

Stimulating plant defense mechanisms to control plant diseases is more advantageous and is becoming an alternative for chemical control mode (Ahmad et al., 2008). *Bacillus* spp. known to activate induced systemic resistance (ISR) in their hosts, which increases host resistance to plant pathogens. *Bacillus amyloliquefaciens* MBI600 induce the synthesis of jasmonic acid (JA), ethylene (ETH), and the regulatory gene *NPR1* in plants (Dimopoulou et al., 2019). The application of *B. amyloliquefaciens* YN201732 increases the host leaves production of phenylalanine ammonialyase (PAL), peroxidase (POD), and improve disease resistance in tobacco (Jiao et al., 2020). It has been reported that *Bacillus subtilis* CPA-8 induces the key signaling molecule of SA and JA defense-related responses in *Monilinia* spp., making them more resistant to peach brown rot (Yanez-Mendizabal et al., 2012). *Bacillus* spp. also enhances the synthesis of defense enzyme activity and *PR* proteins in host tissues in *Nicotiana tabacum* L. this results in increased resistance to mosaic virus, as evidenced by the reduced level of mosaic symptoms observed in plants treated with *B. subtilis* (Ehrenb.) Cohn (Lian

et al., 2011). *Bacillus* Sb4-23 use to mediates ISR in plant hosts through indirect, rather than direct mechanisms, the promote plant growth is often linked with ISR (Etesami & Maheshwari, 2018). *Bacillus pumilus* JK-SX001 has been demonstrated to be an excellent biocontrol agent of *Populus* canker disease caused by three pathogens (*Cytospora chrysosperma* (Pers.) Fr., *Phomopsis macrospora* Chiba., and *Fusicoccum aesculi* Corda.) (Ren et al., 2013). From these literature reviews, *Bacillus* spp. activate ISR in many plants. It is, however, there are few reports on the relationship between *Bacillus* spp. bacteria inducing ISR response pathways in PdPap trees. The interaction between *Bacillus* spp. bacteria and ISR needs to be further elaborated.

The probiotic effect of endophytes *Bacillus* spp. on host plants is achieved by a similar mechanism to ISR (Chen et al., 2020). Many plant endophytes *Bacillus* bacteria isolated from trees, crops, and weeds can thrive inside and outside the plant tissues (Hallmann et al., 1997). For instance, endophytes bacteria *Bacillus aryabhattai* SQU-R12 isolated from *Phoenix dactylifera* L. root and can produce substances such as IAA, ammonia, and acetyl COA carboxylase (ACC) deaminase, which improve *P. dactylifera* growth and have a potential role in salinity tolerance (Yaish et al., 2015). Strain *B. amyloliquefaciens* ZJU1 isolated from the leaves of mulberry tree can significantly reduce the mortality caused by *Botrytis cinerea* Pers.. After inoculation, it can also induce the systemic defense of the plant and cause a high expression of the mulberry disease resistance gene (Xie et al., 2020). Moreover, *Bacillus megaterium* YJB3 promotes the degradation of organic pollutants (Feng et al., 2018), *Paenibacillus* sp. strain B2 is not negatively affected by the impact on the inherent microbial community structure of the soil (Selim et al., 2007). However, *B. amyloliquefaciens* is rarely isolated from the fleshy tap roots of *Brassica rapa* L. Endophytes *Bacillus* spp. isolated from the plant roots are not easily affected by external conditions. Their biocontrol effect on pathogens is more stable than those from plant surfaces (Lopes et al., 2018).

In this regard, we isolated, screened, and identified beneficial endophytes *Bacillus* genus bacteria from fleshy tap root of *B. rapa*. The probiotic effects of endophytes *Bacillus* spp. on PdPap and the induction mechanism of the PdPap defense system were determined using in vitro and the greenhouse.

## Materials and methods

### Bacterial separation and screening

Endophytic bacteria were isolated from the fleshy tap roots of *B. rapa* and screened. The roots were collected from Kashi city, Xinjiang Autonomous Region, China, with geographic coordinates N39° 11′ 42.47″ and E75° 43′ 57.33″. The roots were removed from the soil and were placed in a sterilization bag. They were then loaded into the centrifuge tube containing a constant temperature water bath. The temperature of the water bath was slowly raised to 90 ℃ for 2 h to remove some non-target bacteria that were not heat resistant. After natural cooling, the root surface was disinfected with 7% sodium hypochlorite for 10 min and washed with sterile distilled water three times. The epidermis was excised with a sterile scalpel and cultured on Luria–Bertani (LB) medium to detect the presence of and isolate the bacteria. The internal tissue was chopped, and a small amount of the tissue placed on an LB plate. A 0.5-cm *F. oxysporum* disc was inoculated into the open space of the plate and cultured in a 26 °C constant temperature incubator (Boxun BMJ~400, shanghai, China) under dark conditions for 7 days. Bacteria that produced a distinct zone of inhibition and different colony morphology near the pathogen were selected. The bacteria were placed into fresh LB medium using the point planting method and incubated at 26 °C for 4 days.

In the next step, the dominant bacteria were screened and inoculated into a 0.5-cm-diameter Fox68 fungal disc into the middle of a new PDA plate and cultured for 5 days. The bacteria around the pathogen by streaking method, about 2.5 cm length. The growth of each mycelium was measured after 7 days of incubation at 26 °C in the dark using the cross method (Whipps, 1997). The Fox68 mycelial growth inhibition rate I (%) = ((1 − Dn/Do) × 100, I (%) is the mean inhibition of mycelial growth; Dn is the mean diameter of Fox68 growth in the presence of AW3; Do is the mean diameter of Fox68 growth in the absence of AW3 (control).

One strain with the highest inhibition rate was selected and named AW3. This strain was preserved at the China General Microbiological Culture Collection Center (CGMCC 1.16683). The *F. oxysporum* hyphae at the edge of the confrontation area were selected and observed under a 40× optical microscope. The hyphae were inoculated onto a new PDA plate incubated in a constant temperature incubator at 26 °C for 7 days. Mycelial morphology (curling, thickening, and protoplast lysis), and colony growth status (death and abnormal growth) was observed for a possibility of antagonism (Luna-Bulbarela et al., 2018).

### Identification of strain AW3

To identify the bacteria AW3. DNA was extracted using a DNA kit (Tiangen, Beijing, China) following the manufacturer's recommendations. Amplification of 16S rRNA and the *gyrA* gene were done using methods as described by Yamamoto and Harayama (1995) and Rooney et al. (2009), respectively. The PCR amplification conditions were as follows: Denaturation step of 94 °C for 5 min followed by 30 annealing cycles of 94 °C for 45 s, 55 °C for 45 s, and 72 °C for 1 min and lastly and extension cycle: 72 °C for 10 min. The PCR products were purified and sequenced by Shanghai Sangon Biotech. The sequences were aligned using the National Center for Biotechnology Information (NCBI) Genbank, and the phylogenetic tree was constructed using MEGA7.0 neighbor-joining method (Kumar et al., 2008). The 16S rRNA of all strains was analyzed, and the *gyrA* standard sequence was obtained from the NCBI GenBank database.

### Plant material and fungal strains

This study used potted PdPap seedlings for the test since they are highly susceptible to *F. oxysporum*. PdPap seedlings were differentiated in advance using stem segments and then transferred into 1/2-strength Murashige & Skoog's macronutrient (MS) medium at 25 °C and16 h of light. After growing to 3 to 5 leaves, the roots of the tissue culture seedlings were washed with sterile water and transplanted into 7×7×10 cm bowls containing soil mixture. The soil mixture was made by mixing black soil and vermiculite in a ratio of 7:3 (v/v) and autoclaving at 121 °C for 2 h. Seedlings were cultured in a greenhouse with an air filtration system at 25 °C under a 16L: 8D photoperiod and humidity of 40%. Each bowl was watered once per week with 50 mL.

The *F. oxysporum* CFCC86068 was obtained from the China Forest Culture Collection Center (CFCC). The strain was grown on potato dextrose broth (PDB) plates for 7 days at 26 °C. The liquid PDB medium with the isolated strain was incubated at 28 °C, 160 rpm for 7 days. The concentration based on the ultraviolet spectrophotometer (Eppendorf D30 Germany) $OD_{600}$ value was adjusted to about $1.9 \times 10^8 \sim 2.0 \times 10^8$ (conidia/mL) (Weiss et al., 2014).

### Soil treatment, growth conditions and experimental design

The inoculation methods to verify the control effects of AW3 on PdPap root rot were designed as follows. The control group (water control) was inoculated with 50 mL of sterile water per pot by root irrigation; the treatment group was inoculated *B. amyloliquefaciens* (AW3), and *F. oxysporum* (Fox68) in 50 mL of corresponding fermentation broth with a concentration was $OD_{600}$ $1.8 \times 10^8$ by root irrigation, respectively. In preventive AW3/Fox68 (PRE) treatment, the plants were inoculated with AW3, followed by Fox68. In curative Fox68/AW3 (CUR) treatment group, the plants were inoculated with Fox68, followed by AW3. For co-localization [AW3 + Fox68 (v/v = 1:1)] (COL) treatment, Fox68 and AW3 were simultaneously inoculated, followed by inoculation with Fox68. For PRE, CUR and COL treatments, pathogen fungus (Fox68), or antagonistic (AW3) were inoculated 7 days before the experiments.

The withering degree of the above ground leaves was calculated statistically on a scale from 0 to 4 at 1, 3, 5, 7, and 15 days after inoculation, as previously described by Sánchez Hernández et al. (1998). The scale was based on leaf or flower yellowing or necrosis, where 0 = 0%, 1 = 1% ~ 33%, 2 = 34% ~ 66%, 3 = 67% ~ 100%, 4 = dead plants. The disease index and the control effect were determined based on the degree of disease as described by Evenhuis et al. (1995), using the formulas, Disease index = [∑ (number of diseased plants × representative value)/(total number of plants × representative value of the highest disease level)] × 100%, control effect = (control disease index − treatment of disease index)/(control disease index) × 100.

To verify the promotion effect of AW3 on PdPap, we determined the growth index of PdPap after 15 days of inoculation according to the method used by Sánchez Hernández method (Sánchez Hernández et al., 1998), determine bacterial colonization in roots, stems and leaves by tissue isolation method, and various physiological parameters such as plant weight, plant height, root length recorded.

### Determination of defense-related enzymatic and antioxidant activities after leaf priming with endophyte inoculation

To verify the AW3-induced resistance of PdPap, Evans blue, nitroblue tetrazolium (NBT) staining, and a defense enzyme assay, were performed on PdPap infected leaves. The enzyme method was performed as described by Li et al. (2013). A total of 6~8 leaves of the shoots were randomly collected after inoculation (1, 3, 5, 7, and 15 days). The leaves were transferred to a cold mortar at − 20 °C. Liquid nitrogen was added, and the leaves thoroughly ground. The ground leaf tissue was transferred to a 1.5-mL centrifuge tube using a spatula. A solution of 0.02 M Phosphate buffer was added in a ratio of 1:9 weight of leave tissue to volume phosphate buffer. The mixture was vortexed for 1 min, followed by centrifugation at 3000 rpm for 4 min at 4 °C. A total of 50 μL of the supernatant was transferred into a 5-mL centrifuge tube. Following the procedures of the enzyme activity kit (NJJCBIO, Nanjing, China), the agent was added to the control tube and the measuring tube and vortexed thoroughly to determine the colorimetric absorbance (Eppendorf D30, Berlin, Germany).

On the 15th day, 6~8 leaves were taken from the plant. As described by Lin et al. (2005), the leaves were soaked in Evans Blue dye solution [1% (w/v)] for 15 min in the dark. They were then transferred into a 50-mL centrifuge tube containing 75% ethanol, 5% glycerol, and 20% distilled water. Under the catalysis of peroxidase, $H_2O_2$ can quickly react with DAB to generate brown compounds, thereby locating $H_2O_2$ in the tissue. NBT staining was done using the Romero-Puertas method (Romero-Puertas et al., 2004); The leaves were placed in the NBT dye solution [0.1% (w/v)] for 8 h. NBT is reduced to water-insoluble blue dimethyl under the action of O-, Blue staining indicated that cell death had occurred. Statistical analysis of Evans blue (top) and NBT (bottom) results were performed using ImageJ1.52p software.

## RNA extraction and relative gene expression quantification by reverse transcription RT-qPCR

To determine whether AW3 enhanced the molecular mechanism of PdPap disease resistance, expression of gene related to plant disease resistance and hormone signaling was determined using RT-qPCR. After inoculation for 6, 12, 24, 36, and 48 h, 10 randomly PdPap roots were collected and mixed with 0.9% saline in A 5-mL centrifuge tube. The tube was quickly frozen in liquid nitrogen and stored in a freezer at – 80 °C for use. RNA was extracted using the Plant RNA Extraction Kit (BIOTEKE, Beijing, China). The extracted RNA was assayed for RNA concentration using a UV spectrophotometer (BIOTEKE ND5000) ($OD_{260/280}$), and quality mass determined using 2% TAE agarose electrophoresis. The RNA was diluted with diethylpyrocarbonate (DEPC) water to a final concentration of 1 ug, and single-strand cDNA was synthesized using a PrimeScript$^{TM}$ RT reagent Kit with gDNA Eraser (Takara, Tōkyō, Japan). The RT-qPCR primers are shown (Table S1). The assay was carried out in a 25 μL reaction mixture containing 12.5 μL SYBR® Premix Dimer Eraser$^{TM}$, 0.75 μM primer, 11 μL of 100 ng cDNA, and water. The qPCR assay was performed using the RT-qPCR detection system (Agilent Mx3000P, California, USA). The following conditions were used: 95 °C for 10 s, and then 40 cycles of 95 °C for 10 s, 55 °C for 30 s, and 72 °C for 30 s. *ACT* and *TUB* were used as housekeeping genes to standardize results. The gene expression related was calculated relative to the control using the $2^{-\Delta\Delta Ct}$ method, as described by Livak and Schmittgen (2001).

## SEM observation

SEM was used to observe the morphology of the root surface to understand the AW3 strain better biological competitiveness ability in PdPap roots. After 15 days inoculation, the roots were washed with sterile water and photographed. The roots of each treatment group were cut into 3- to 4-mm sections using a sterile scalpel. The root sections were fixed with 1% glutaraldehyde as described by Boukaew et al. (2013), and ethanol used for stepwise dehydration. The morphology of the inferior root surface inoculum was observed using an electron microscope (JSM-7500F, Tōkyō, Japan) and treated with water as a control.

## Statistical analyses

All the experiments were repeated at least three times and data obtained were statistically analyses with Origin 2018 (Learning Edition). The treatment and the control group were compared multiple times by using one-way analysis of variance (ANOVA). The significance of differences amongst all treatments were tested using Duncan multiple range test at *P* values of<0.05.

## Results

### Antagonistic effect of biocontrol bacteria AW3 to mycelial growth of Fox68

We isolated by the plate confrontation screening to get a strain of AW3 from fleshy tap roots of *B. rapa*. After 7 days of co-culturing with Fox68, a significant inhibition zone appeared (Fig. 1B). A high inhibition rate with a maximum of 79% was observed (Fig. 1E). The difference was extremely significant (Fig. 1A). For a better understanding of the antagonistic effect of AW3 on Fox68, the edge hyphae of Fox68 (Fig. 1B, white arrow) were selected and observed under an optical microscope. Compared with the control (Fig. 1C), the Fox68 mycelium cultured with AW3 was ruptured, thickened, twisted, and enlarged at the tip (Fig. 1D black arrow). When the hyphae were inoculated onto a new potato dextrose agar (PDA) plate, and cultured for 7 days, the hyphae failed to grow.

### Strain identification of AW3

The identification of strain AW3. The colony morphology of strain AW3 was nearly circular, smooth, and milky white when cultured on LB agar medium for 24 h. The cellular morphology of strain AW3 was rod-shaped. Its colony and cellular morphology have been shown in (Fig. 1F, H). On molecular aspects, the 16S rDNA and *gyrA* gene fragments of AW3 genomic DNA were 1400 bp and 740 bp in size, respectively. They were deposited at the National Center for Biotechnology Information (NCBI and assigned accession numbers MK228853 and MK396079. Strain AW3 belonged to the same genus branch as *B. amyloliquefaciens* (NR118950.1)
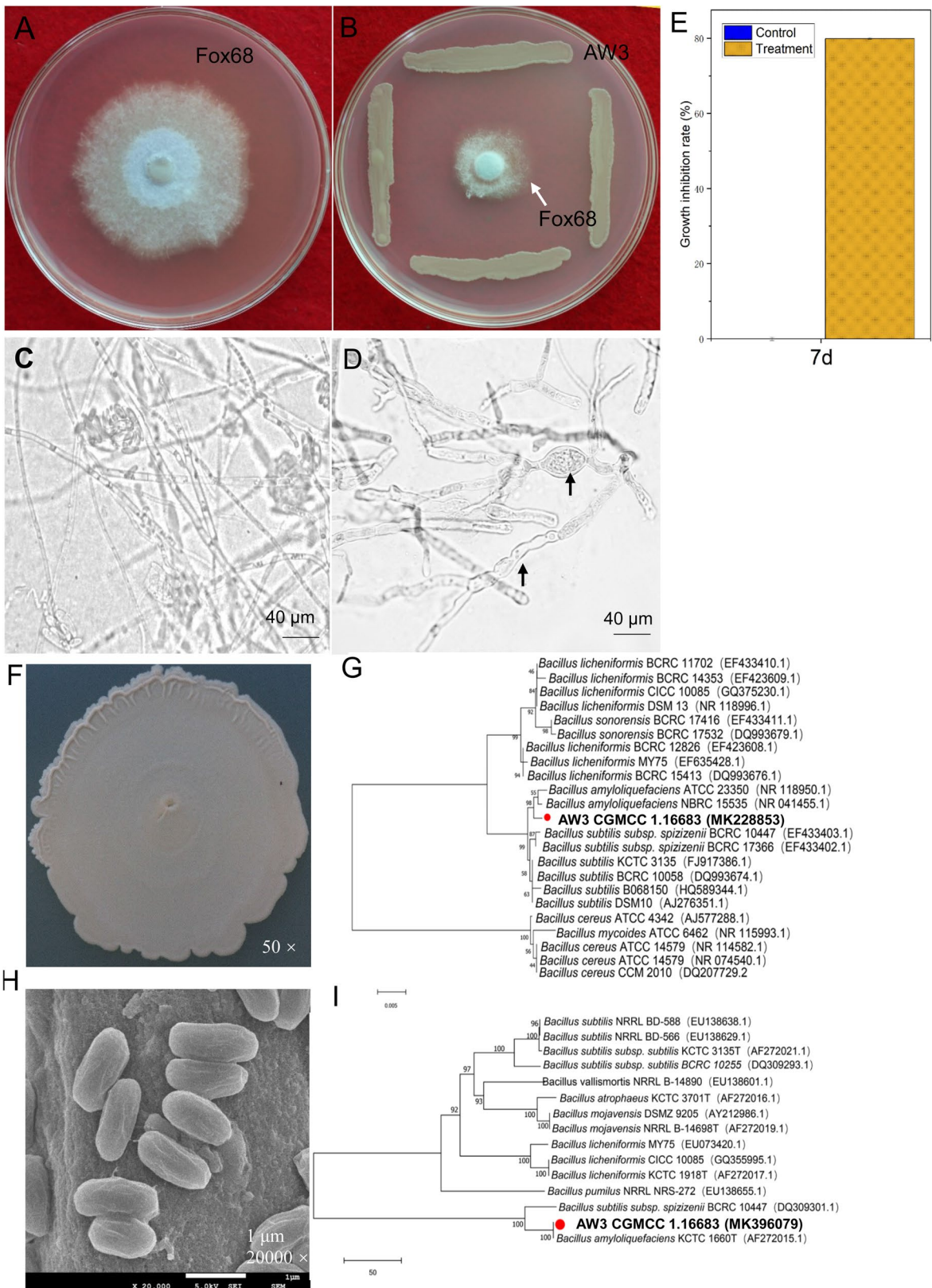
◄**Fig. 1** The effect of strain AW3 on the colony growth inhibition rate of Fox68. **A** The Fox68 colony was cultured separately in the PDA medium. **B** The colony morphology of the cultivars cultured in the PDA medium simultaneously inoculated with Fox68 and AW3. **C** Observation of morphological characteristics of Fox68 (white arrow) mycelium using an optical microscope. **D** Fox68 and AW3 morphological characteristics of mycelium after cultivation (black arrow). **E** The average colony diameter of Fox68 (6 biological replicates) after confrontation culture measured using the cross method. **F** Colony morphology (LB agar medium). **G** Observation of cellular morphology using a SEM and NJ tree showing the phylogenetic positions of strain AW3 and other related taxa based on 16S rRNA (**H**) and *gyrA* (**I**) gene sequences. Bootstrap values (expressed as percentages of 1000 replicates) shown at branch points. Bar, 0.005-nt substitution rate. All the culture conditions were incubated in the dark at 25 °C for 7 days, during plate confrontation, all plates were always cultured until the fungus in control plate grew to full plate, then the inhibition rate was measured and calculated

and *B. amyloliquefaciens* (NR041455.1) exhibiting the closest genetic distance to *B. amyloliquefaciens* (NR041455.1), with a support rate of 98% (Fig. 1G).

The *gyrA* genes were amplified and sequenced for further characterization of AW3. Standard strain sequences were downloaded from the NCBI online alignment website. Using MEGA 7 to construct a phylogenetic tree, the closest genetic distance of AW3 sequences to *B. amyloliquefaciens* (AF272015.1) was 100% (Fig. 1I). The 16S rDNA phylogenetic tree showed the same results as the *gyrA* gene. Therefore, the strain AW3 was identified as *B. amyloliquefaciens* by both morphological and molecular characterization.

### The effect of endophyte AW3 on the control of *Fusarium* root rot disease in PdPap seedlings

We determined the effect of endophyte AW3 on the control of *Fusarium* root rot in PdPap seedlings. A pathogenicity test showed that Fox68 was pathogenic to PdPap. The plant performance revealed the symptoms commonly observed in the nursery. For instance, the upper part of the leaves yellowed and withered, and eventually, whole plants were dead (Fig. 2A3). The parts below the ground decayed, and the epidermis fell off (Fig. 2B3), and the PdPap seedlings began to die after the 15th day of infection. In the preventive (PRE) treatment group, after 15 days of inoculation, the disease index of PdPap disease decreased by 41% compared with Fox68 alone (Fig. 3A); only leaves at

the bottom part of the stem wilted (Fig. 2A4), and there was no decay in the roots (Fig. 2B4). In the curative (CUR) treatment group, the symptoms of the above-ground parts did not progress (Fig. 2A5). After 15 days, the disease index had decreased by 11% compared with Fox68 alone, and the degree of root rot slowed (Fig. 3). New root growth (Fig. 2, yellow arrow) and new leaves began to appear in the upper part. In the co-localization (COL) treatment group, there were no obvious symptoms on the shoots above and below the ground (Fig. 2A6, B6), and the control effect on the 15th day was 55% and 61% higher than those of the PRE and CUR treatment groups respectively (Fig. 3B).

### The growth promotion function of endophyte AW3 to PdPap seedlings

We determined the growth promotion effect of endophytes *B. amyloliquefaciens* AW3 on PdPap seedlings. The results (Table 1) showed the following. In the COL treatment group, the fresh weight and dry weight of the leaves were significantly higher than those in the water control, by 15.71 and 1.42 g, respectively. Among three indicators (leaf width, leaf length, and plant height), the COL treatment group was the most significant. Compared with the water control, the three indicators (leaf width, leaf length, and plant height) showed a positive response, with increases of 2.26, 2.70, and 4.45 cm, respectively. In the Fox68 treatment alone, leaf length and leaf width were 1.45 and 0.76 cm lower, respectively, than those in the water control. The lowest plant height was measured in the CUR treatment group, which was 2.6 cm lower than that of the water control. The root number and length differed significantly among the treatment groups. The COL treatment group had the highest number of roots, approximately 198 more than the water control. The Fox68 treatment group had the fewest number of roots, about 22 fewer than the water control. The same results were observed for the root length index, and the total length of the COL treatment group was the greatest, i.e., 8.08 cm longer than that of the water control.

### Antioxidant activities caused by priming PdPap seedlings with endophyte AW3

We investigated the levels of antioxidant activities after priming PdPap seedlings with endophyte
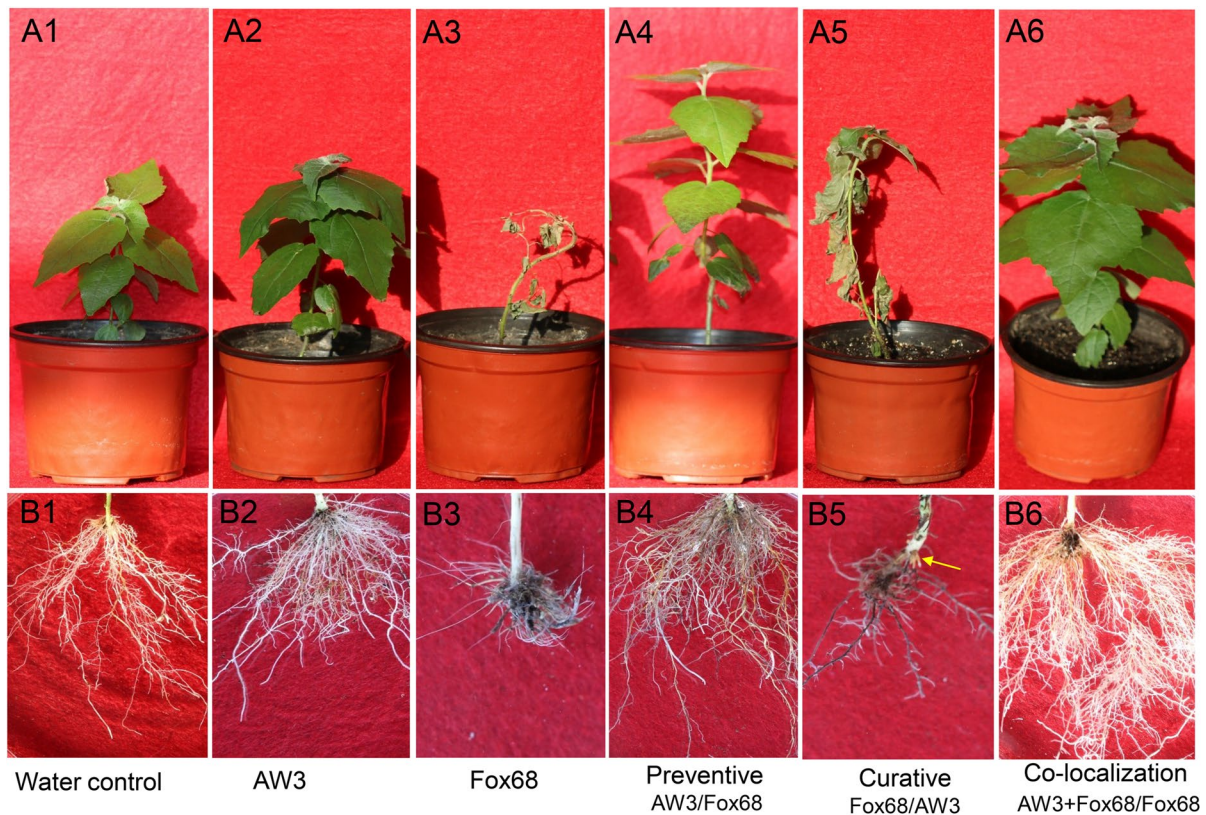
**Fig. 2** Symptoms of PdPap root rot after inoculation with Fox68 and AW3 for 15 days. **A1**, **B1** Water control. **A2**, **B2** *B. amyloliquefaciens* (AW3) inoculated plants. **A3**, **B3** *F. oxysporum* (Fox68) inoculated only with Fox68. **A4**, **B4** Preventive AW3/Fox68 (PRE) treatment: Fox68 was inoculated after the AW3 inoculation of the plants. **A5**, **B5**. Curative Fox68/AW3 (CUR) treatment: The plants were inoculated with Fox68, fol-lowed by AW3. **A6**, **B6** Co-localization AW3 + Fox68/Fox68 (COL) treatment: Fox68 and AW3 were simultaneously inoculated followed by inoculation with Fox68. PRE,CUR and COL treatment were inoculated 7 days prior with pathogen (Fox68) fungus or antagonistic (AW3) bacteria. All the plants were inoculated in the roots; 25 strains per treatment, Biological 3 replicates

AW3. The staining area in leaves subjected to Fox68 was higher than that of leaves inoculated with AW3 and the water control (Fig. 4A), with a significant difference (Fig. 4B). The necrotic area of the leaves was greater in the PRE, CUR, and COL treatment groups than in the inoculated AW3 and water controls. Moreover, necrosis occurred in the leaves of the Fox68, PRE, CUR, and COL treatment groups. The difference in the leaf necrosis area between the PRE and Fox68 treatment groups was not significant, whereas the necrotic area in the COL and CUR treatment groups was lower than that in the PRE group.

### Defense-related enzymatic activities caused by priming PdPap seedlings with endophyte AW3

We investigated the levels of defense-related enzymatic activities after priming PdPap seedlings with endophyte AW3. The first was the CAT and PAL enzyme, the CAT enzyme had the highest activity on the 15th day in the COL treatment group, which was 2.59 times higher than that of the water control. In response to the single inoculation of Fox68, the CAT enzyme was the most active in all treatment groups on the 3rd day, which was 2.64 times higher than that in the water control. The CAT enzyme activity in
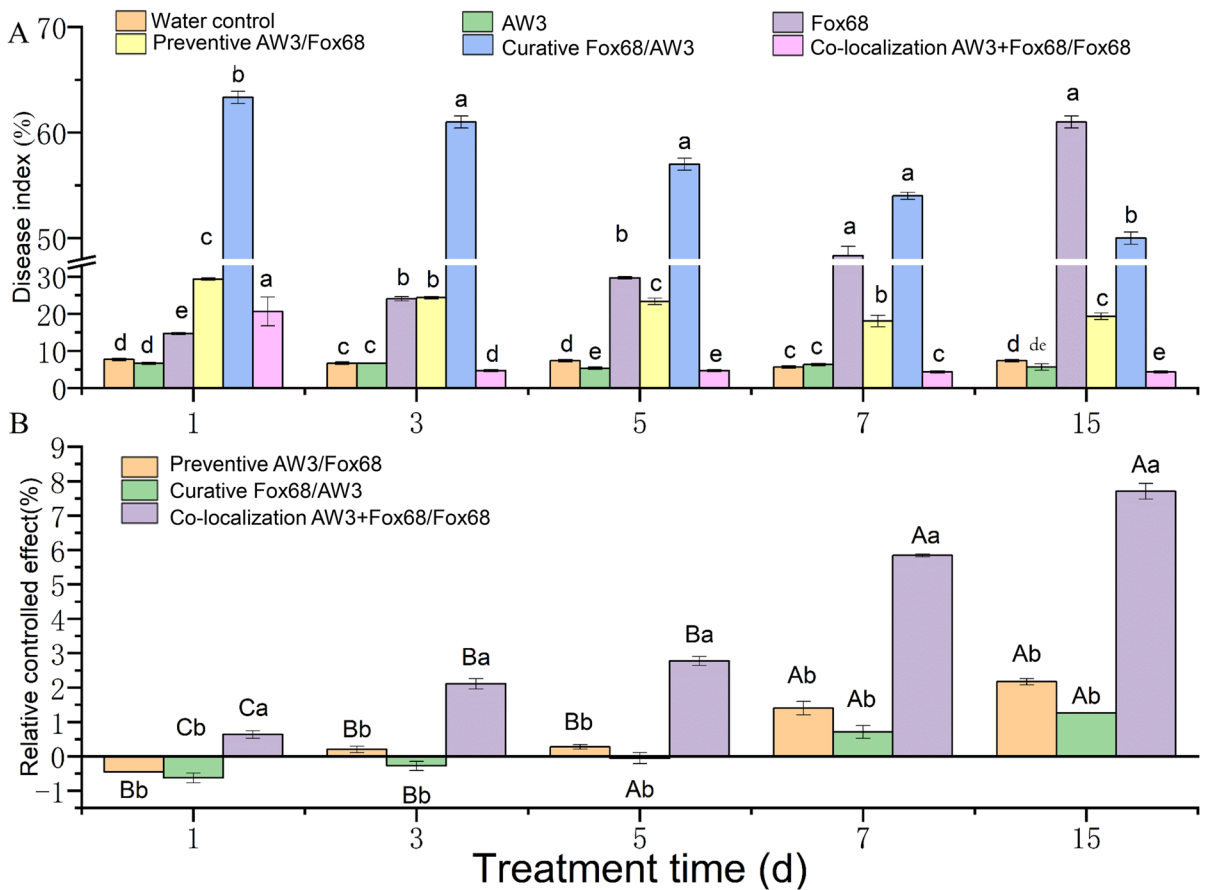
**Fig. 3** Severity index of PdPap root rot under different inoculation methods. **A** The upper part of the disease index of PdPap root rot on the water control, AW3 (*B. amyloliquefaciens* (AW3) inoculated plants), Fox68 (*F. oxysporum* (Fox68) inoculated plants), Preventive AW3/Fox68 (PRE) (AW3 treated plants followed by Fox68 infestation), Curative Fox68/AW3 (CUR) (Fox68 infested plants treated with AW3), and Co-localization AW3+Fox68/Fox68 (COL) (Fox68 and AW3 were simultaneously inoculated followed by inoculation with Fox68). **B** Relative control effect of PdPap root rot after 15 days of combined inoculation. Different lowercase letters indicate significant differences between the groups at the same time point, and the different uppercase letters indicate significant differences for the same treatment group at different times. Error bars represent standard errors of the mean (n = 3) at each time point; The combined inoculation was repeated after inoculation of the pathogen (Fox68) fungus or antagonistic (AW3) bacteria for 7 days, and all of the plants were inoculated in the roots; Biological 3 replicates were done per treatment

AW3, PRE, CUR, and COL increased from day 1 to 15, while from day 1 to 5, the CAT enzyme activity of Fox68 increased first and then decreased (Fig. 5A). Similarly, PAL enzyme activity in the COL treatment group was the highest on day 15, which was 1.77 times higher than that of the water control. In addition, the Fox68 treatment group was the most positive among all groups on day 15, and 0.97 times lower than the water control. The overall effect of AW3 from day 1 to 15 tended to be moderate, and the difference was not significant compared with other time points. From day 1 to 3, there was a slight increase in enzyme activity response to Fox68, followed by a decline from day 3 to 15. The trend from day 1 to 15 in the PRE and CUR treatment groups was not obvious, but PAL enzyme activity in the PRE treatment group was higher than that in the water control (Fig. 5B).

The second was the POD enzyme, POD enzyme had the highest activity on day 3 in the COL treatment group. The POD enzyme activity was 2.97 times higher than that of the water control, and the

**Table 1** Effect of AW3 on growth parameters and plant mortality of PdPap inoculated with Fox68

| Treatments | Leaf fresh mass (g plant⁻¹) | Leaf dry mass (g plant⁻¹) | Root number | Root length (cm) | Leaf length (cm) | Leafs width (cm) | Plant height (cm) |
|---|---|---|---|---|---|---|---|
| Water control | 15±1.97d | 3.89±0.52b | 77.0±0.45d | 5.34±0.64 e | 2.67±0.28c | 1.65±0.22d | 7.03±0.51bc |
| AW3 | 18.82±2.75c | 3.79±0.41b | 143.4±1.22c | 6.1±0.38 d | 3.08±0.24c | 2.94±0.16c | 7.07±0.27bc |
| Fox68 | 9.62±1.02f | 3.55±0.20b | 45.06±7.48e | 2.86±0.36 f | 1.20±0.39d | 0.89±0.19e | 6.52±0.86c |
| PRE (AW3/ Fox68) | 22.30±2.33b | 3.52±0.21b | 190.47±9.28b | 7.81±0.67 c | 4.08±0.38b | 3.36±0.21b | 7.30±0.59b |
| CUR (Fox68/ AW3) | 11.42±0.30e | 2.82±0.39c | 51.00±1.48e | 9.37±0.99 b | 2.83±0.22c | 1.74±0.19d | 4.43±0.52d |
| COL(AW3+ Fox68) | 30.71±2.70a | 5.31±1.11a | 276.41±1.64a | 13.42±1.48 a | 4.93±1.32a | 4.35±0.30a | 11.48±1.36a |

Results are the mean of six replicates with ± standard error (SE). Means followed by the same letter (s) within a column are not significantly different according to Duncan's test (*P*< 0.05)

POD enzyme activity began to decrease from day 3 to 15. The Fox68 inoculation alone resulted in an overall increasing trend from day 1 to 15. In the PRE, CUR, and COL treatments, the activities of the three enzymes generally increased first and then decreased (Fig. 5C).

The second was the SOD enzyme, SOD enzyme increased from day 1 to 3 of the AW3 treatment and then stabilized from day 3 to 15. The Fox68 treatment showed a positive response from day 1 to 3, and then a negative response after day 3. The SOD enzyme activity on day 1 was the highest in Fox68 and PRE, i.e., 1.67 and 1.60 times higher, respectively, than that in the water control. On day 15, the highest SOD enzyme activity was observed in PRE and COL, i.e., 1.70 and 1.68 times higher, respectively, than in the water control (Fig. 5D).

Differential expression of PdPap gene related to SA and JA signal transduction pathway inducing by endophyte AW3

We determined the differential expression of the PdPap gene associated with the SA and JA signal transduction pathway induced by endophyte AW3. The first was the salicylic acid (SA) pathway. The *PR1* gene was up-regulated under AW3-induced inoculation, and the transcription peak was 3.50 times higher than that of the water control group (Table S4), while the gene of the Fox68 treatment group was down-regulated. The peak of transcription was the greatest in the PRE treatment group,

which was 5.12 times higher than that of the water control. The CUR and COL treatment groups were downregulated after 6 h and 24 h, and they were 1.23 and 1.55 times lower, respectively, than the water control group (Fig. 6A). Compared with the *NPR1* gene in the water control group, allgenes were upregulated from 6 to 12 h. The highest upregulation was in the PRE treatment group, which was 2.13 times higher than that of the water control. The *PR1* and *NPR1* genes were downregulated in Fox68 alone compared to the water control and showed small fluctuations in AW3 alone (Fig. 6B).

Moreover, AW3 significantly induced the transcription of the JA pathway gene. The *MYC2* and *JAR1* genes of strains AW3 and Fox68 had up-regulated peaks at 24 h; they were 4.17, 4.92, 6.92, and 7.45 times higher than those in the water control group (Fig. 6C, E). The *JAZ6571* gene was downregulated. The maximum peak of AW3 transcription was 2.23 times higher than that of the water control group, and the transcription peak of Fox68 was 3.51 times higher than that of the water control (Fig. 6D). The *MYC2* and *JAR1* genes were upregulated. The maximum transcription peaks of the *JAR1* gene in the three treatment groups, PRE, CUR, and COL, were 7.87, 8.07, and 7.76 times higher, respectively, than those in the water control group. In the PRE, CUR, and COL treatment groups, the *JAZ6571* gene was upregulated from 6 to 24 h. After 24 to 48 h, downward adjustment occurred. The maximum peak values of the downregulated transcription were
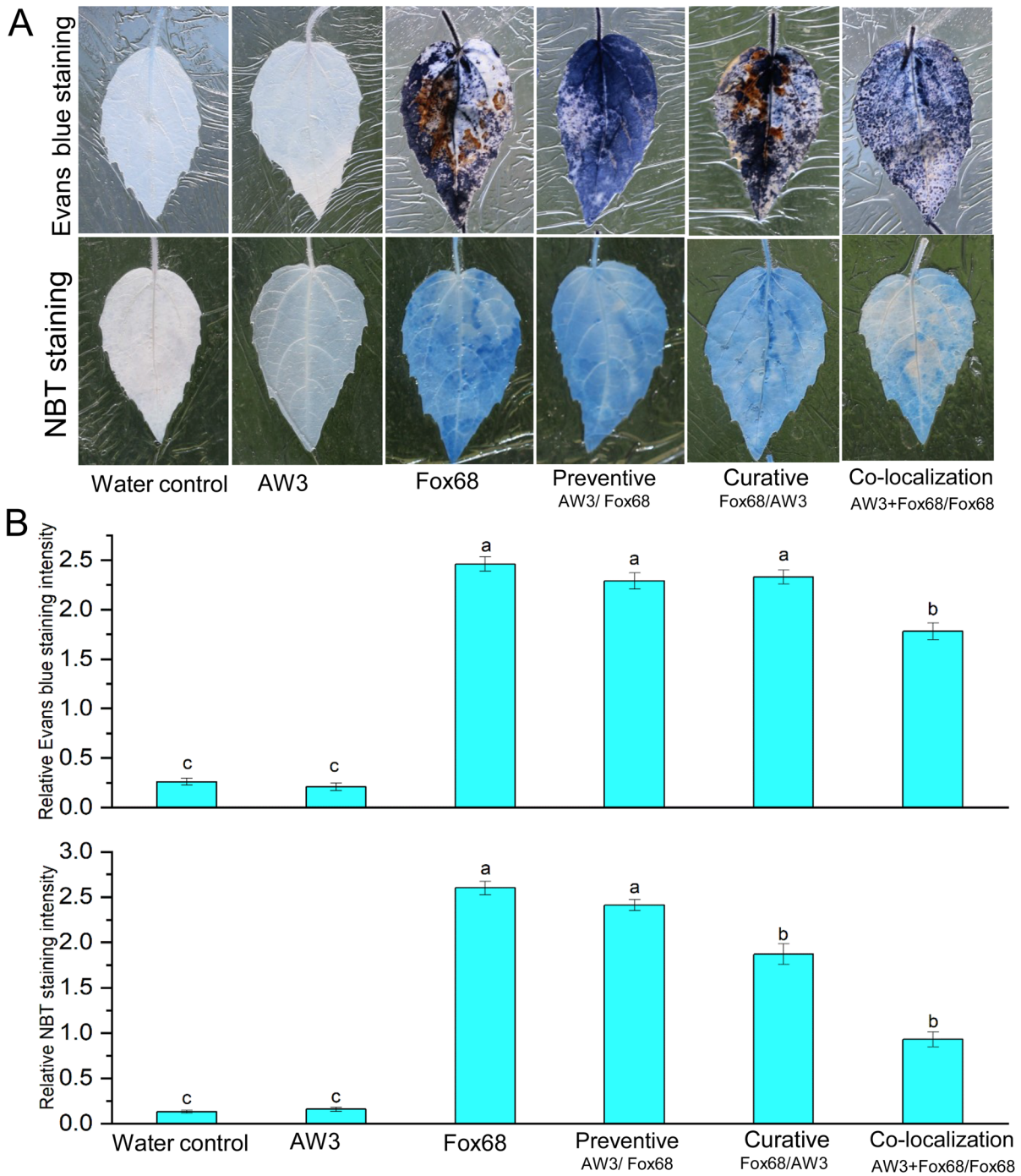
**Fig. 4** Evans blue and NBT staining used to detect the degree of necrosis and $O_3$ levels in the differently treated cells. **A** Shows the results of leaf staining with Evans blue and NBT after 15 days of treatment [water control, AW3, Fox68, preventive AW3/Fox68 (PRE), curative Fox68/AW3 (CUE), co-localization AW3+Fox68/Fox68 COL)]. **B** Statistical analysis of Evans blue (top) and NBT (bottom) using ImageJ software. The bar graph number represents the mean of 4 values. The a, b, and c indicate significant differences between treatments. Error bars represent standard errors of the mean (n=4) at each time point
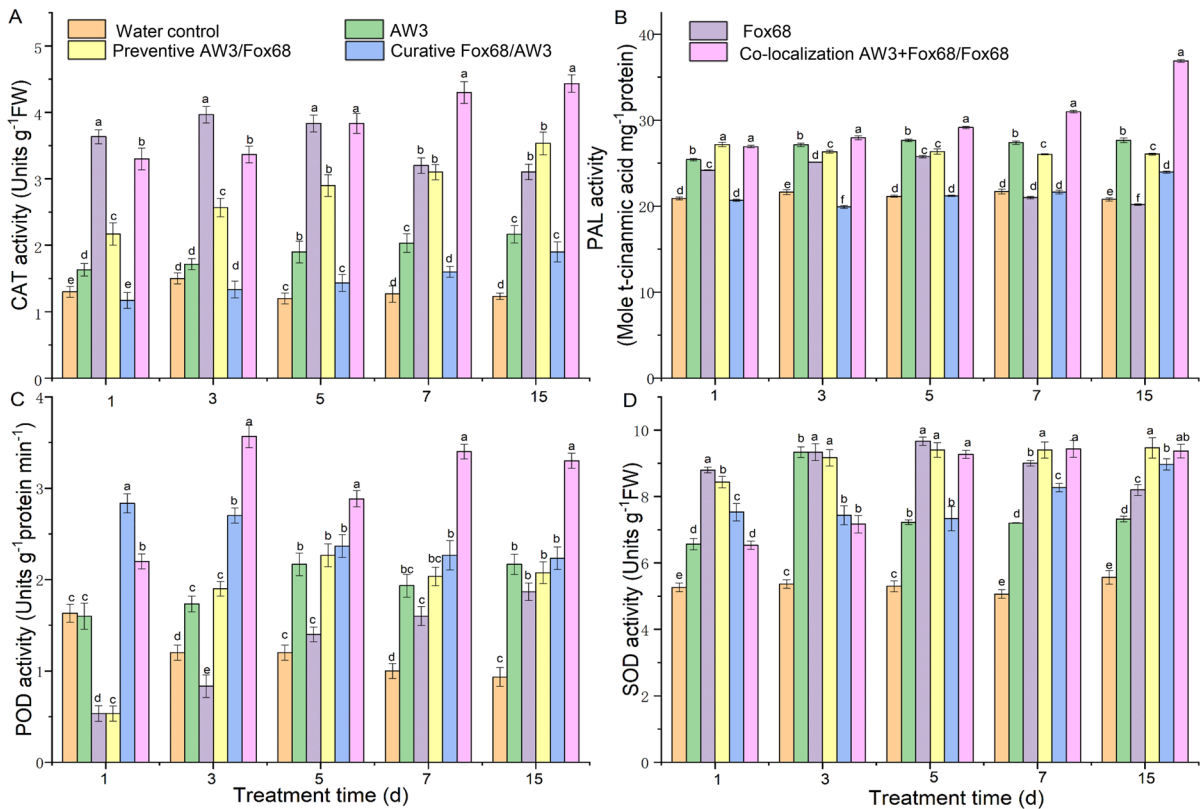
**Fig. 5** Defense enzymatic activities in PdPap leaves using different inoculation methods. **A** Catalase (CAT). **B** Phenylalanine ammonia-lyase (PAL). **C** Peroxidase (POD). **D** Superoxide dismutase (SOD). The graphical values are the average of 4 biological repeats. Error bars represent standard errors of the mean (n=4) at each time point. The a, b, and c indicate a significant difference between treatments

3.32, 2.94, and 3.57 times higher than that of the water control.

AW3 clearly induced the transcription of auxin signaling-related genes. Transcription of *MP*, *AUX1*, and *LAX2* genes (Fig. 6F, G, H) was down-regulated compared with the water control from 6 to 12 h and then began to be upregulated after 12 to 48 h. The maximum upregulated transcription peaks of the *AUX1*, *LAX2*, and *MP* genes in the AW3 treatment groups were 3.33, 2.34, and 2.82 higher, respectively, than those of the water control group. The maximum peaks of the transcription of *AUX1* genes in the PRE, CUR, and COL treatment groups were 2.88, 2.93, and 2.51 times higher, respectively, than those of the water control. The maximum peaks of the transcription of *LAX2* genes in the PRE, CUR, and COL treatment groups were 2.95, 3.31, and 2.73 times higher, respectively, than those of the water control.

### Interacting Fox68 with endophyte AW3 by SEM observation

In this section, the biological competitive ability of strains AW3 and Fox68 in PdPap roots were determined. For the water control, the root surface was smooth, there was no visible damage, and no hyphae were observed (Fig. 7A1, A2). Moreover, no mycelium was observed on the root surface indicating that the PdPap was not contaminated by other microorganisms during growth. The AW3 strain was distributed in the gap between the surface of the PdPap root during the inoculation process (Fig. 7B1, B2), and the root surface was smooth with no visible damage. During Fox68 inoculation, several hyphae were attached to the root surface, no spores were observed, and the root surface was damaged (Fig. 7C1, C2). In the PRE treatment group, a small amount of Fox68 hyphae adhered to the root surface, and the root epidermis
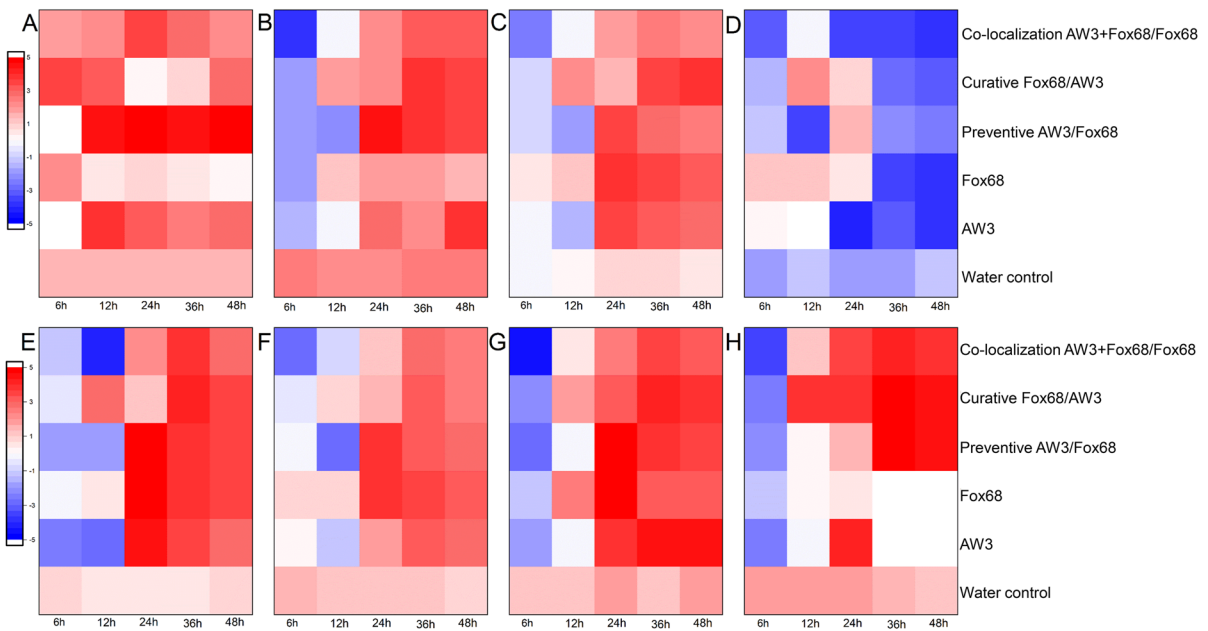
**Fig. 6** Heat map of gene expression associated with the defense of PdPap roots. A and B represent the expression of *PR1* and *NPR1* respectively in the SA signal transduction pathway; C, D, and E represent the expression of *MYC2*, *JAZ6751*, and *JAR1* respectively in the JA signal transduction pathway; F, G, and H represent the expression of *MP*, *AUX1*, and *LAX2* respectively in the auxin signal transduction pathway. All the experiments were performed 4 times
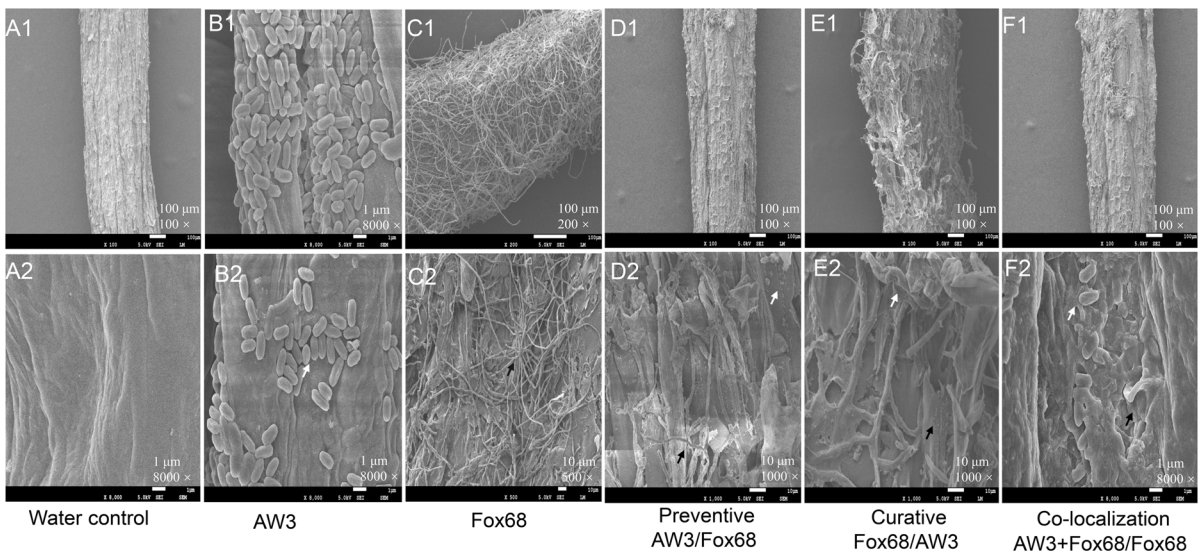


**Fig. 7** SEM observation of hyphal and epidermal morphology of the root surface after inoculation. (**A1**, **A2**) Uninoculated. (**B1**, **B2**) Inoculated with AW3. (**C1**, **C2**) Inoculated with Fox68. (**D1**, **D2**) Initial inoculation with AW3, late inoculation with Fox68. (**E1**, **E2**) Initial inoculation with Fox68; late inoc- ulation with AW3. (**F1**, **F2**) Fox68 and AW3 were simultane- ously inoculated, and then later inoculated with Fox68. Fox68 and AW3 are represented by black and white arrows respec- tively. Each treatment performed in triplicate and three plants were randomly selected for each repetition

had low damage than in the Fox68 treatment. Notably, the hyphae morphology showed thickening, rupture, and internode shortening, and AW3 was distributed on the mycelium (Fig. 7D1, D2). Besides, in the CUR treatment group, the root epidermis was damaged, Fox68 hyphae showed breakage and thickening, and AW3 was visible on the mycelium surface (Fig. 7E1, E2). Similarly, the PRE treatment group hyphae were lower than that in the Fox68 treatment group. In the COL treatment group, the hyphae were highly thickened and twisted and the morphological structure was difficult to distinguish compared with PRE and CUR groups. A small amount of AW3 was observed on the mycelium surface (Fig. 7F1, F2).

## Discussion

*Bacillus* bacteria have several antagonistic properties. They play an important role in promoting plant growth and inhibiting disease by colonizing the surface or inner root tissues (Etesami & Alikhani, 2016). Methods for screening for effective bacteria strains and understand the underlying biological control mechanisms are important for controlling plant diseases. Microorganisms or metabolites have traditionally been used to control plant pathogens and may substitute chemical control methods (Fravel, 2005). In this study, the endophytes bacteria from the *Brassica rapa* roots were isolated, using 90 ℃ high temperature to remove some non-target bacteria and selected some strains with antagonistic ability to pathogenic fungi. Among all the PGPR species, *Bacillus* species are considered a highly effective group because they produce persistent spores under adverse environmental conditions (Nazari & Smith, 2020; Tashi-Oshnoei et al., 2017). Besides, the AW3 strain is not pathogenic to tobacco and PdPap (Fig. S2) and can be re-isolated from PdPap (Table S3). The AW3 isolate lacks specificity for plant hosts. Although PdPap and *B. rapa* are different in terms of most characteristics, they grow in a harsh environment at high temperatures. Other studies have reported that it is more advantageous to use biological control agents that can co-evolve or are compatible with the host (van Loon, 2007).

Bacteriostatic action is an important mechanism for controlling root rot using *Bacillus*. A study by Zhang et al. found that *B. subtilis* KB~1122 can cause *Magnaporthe oryzae* P131 mycelial cell malformation, swelling, distortion, and deformation (Zhang et al., 2014). In the confrontation training, we observed that the Fox68 hyphae were characterized by thickening, tip expansion, and internode shortening. The mycelial growth of the fungus was significantly reduced by 79% after 7 days. Our research results are consistent with the reported research results. However, under natural conditions, AW3 and Fox68 usually coexist in soil. The antagonistic efficiency of AW3 depends on the number of pathogens, nutrition, and environmental conditions in the soil. Therefore, we transferred the experiment from the plate to potted seedlings in the greenhouse to determine the antagonistic effect of AW3 in the soil. The results showed that AW3 can antagonize Fox68 in soil using scanning electron microscopy. Similarly, the results from observations supported the findings of Zhang *et al* (Zhang et al., 2014).

Besides, the induction of defense enzyme expression in host plants is an important biocontrol mechanism used by *Bacillus* to control plant diseases (Srikhong et al., 2018) For example, PO and PPO activity is responsible for phenol oxidation, strengthening the cell barrier (Peng, 1992). Another PAL enzyme initiates the phenylpropanoid pathway, resulting in the biosynthesis of phytoalexins or phenolic compounds. Some studies have shown that activation of the phenylpropanoid pathway protects plants from pathogen infection (Ors et al., 2019). However, increased activities of the four enzymes observed in AW3-treated PdPap plants significantly reduced the disease index and promoted PdPap growth. These results are consistent with a report by Schmitt et al. (2014). Furthermore, we reported that AW3 either alone or in combination with *F. oxysporum* could induce PdPap defense mechanisms and reduce the disease level. Similar studies subjected the pathogen *Phytophthora capsici* to stress conditions and reported an increase in PPO activity in response to the co-inoculation of actinomycetes (Yang et al., 2010).

Current studies have reported that reactive oxygen species (ROS) produced in plants under various biotic and abiotic stresses cause oxidative stress (Ivanova et al., 2021). When ROS production and antioxidant defenses are out of balance, this leads to oxidative stress response. Plants have a variety of complex cellular defense mechanisms to protect themselves from plant pathogens. In this study, under Fox68 stress,

the activity of PdPap defense enzymes increased in the presence of AW3, and the area of leaf necrosis indicated by Evans blue and NBT decreased. In the early host response to pathogen attack, the resulting superoxide radicals rapidly clear $H_2O_2$. Therefore, the released $H_2O_2$ can promote the structural enhancement of the plant cell membrane by defending enzyme activity (Schmitt et al., 2014). This study again confirmed that AW3 triggers a change in the activity of the relevant defense enzymes when used as a treatment for PdPap, which resulted in a reduction of ROS and eliminated excess free radicals. Therefore, the use of organisms to induce a systemic level of resistance to a pathogen by a plant prior to infection with a pathogen can reduce mortality caused by the disease. In some similar reports, ROS accumulation is considered one of the main responses in gramineous plants; it starts from the biotrophic stage and spreads to the whole leaf tissue in the late stage (Yang et al., 2015) In this study, it was found that AW3 can induce the increase of antioxidant enzyme activity in PdPap trees to resist the invasion of pathogens.

AW3 reactivates the signaling pathways that respond to plant hormone-related genes, such as JA and SA. It plays a key role in regulating plant defense pathways, mainly based on a complex network regulation in the absence of host-pathogen interactions (Wu et al., 2018). Results from this study indicated that the *PR1* and *NPR1* genes of the salicylate pathway were significantly upregulated with AW3 inoculation. Notably, after Fox68 infection with, *NPR1* and *PR1* were oppositely downregulated. It was observed that the AW3 strain re-induced the expression of PdPap *NPR1* and *PR1* genes. Also, *MYC2*, *JAR1,* and *JAZ6751* genes for the JA pathway were downregulated through AW3 and Fox68 induction. This may be attributed to the nutritional characteristics, hosts for Fox68 and AW3, or synergy the SAR and ISR pathways (Cameron et al., 2013). Similar findings have shown that the *NPR1* gene mediates plant ISR pathway through synergy after infection by znonpathogenic bacteria (Anderson et al., 2004). Besides, subsequent research found that *NPR1* mediates SAR in SA and mediates ISR induced by JA (Fan & Dong, 2002). Co-inoculating AW3 and Fox68 highly accelerate the SA/JA signaling pathway. This phenomenon may partly explain why PdPap is highly resistant to Fox68 infection. Based on the transcriptional trends, all three genes (*AUX1, MP,* and *LAX2*) were upregulated compared to water control. In a similar study, the *AUX1* gene showed the same results when *Bacillus* was used on *Arabidopsis thaliana* (Wang et al., 2015). To sum up, AW3 affected the JA and SA signal transduction pathways of PdPap causing ISR and SAR. Therefore, gene expression associated with auxin signaling should be induced to promote the growth of PdPaps to ensure broad-spectrum PdPap resistance to pathogens.

In summary, under the biological stress of Fox68, AW3 directly acted on the hyphae of Fox68, reducing the disease of PdPap caused by Fox68. Moreover, AW3 can confer resistance by inducing the accumulation of defense-related enzymes/genes. The combined effect of related defense enzymes and genes lowers the disease index of PdPap. Therefore, findings from this study highlight the critical role of AW3 in inhibiting the PdPaps pathogenesis after infection with the Fox68 pathogen. Overall, the study reported that molecular mechanisms are involved in host resistance to *F. oxysporum* infection through endophytes induction. This may be vital in applying AW3 under field conditions to control PdPaps. However, additional knowledge is required to understand how to trigger signal transduction of PdPap in combined inoculation. This will be the focus of our next study.

**Declarations**

**Ethical approval** All authors have read and approved the final manuscript. This manuscript is not under consideration by another journal and has not been previously published. This article does not contain any studies with animals performed by any of the authors.

# References

Ahmad, P., Sarwat, M., & Sharma, S. (2008). Reactive oxygen species, antioxidants and signaling in plants. *Journal of Plant Biology, 51*(3), 167–173.

Anderson, J. P., Schenk, P. M., Desmond, O. J., Maclean, D. J., Ebert, P. R., & Kazan, K. (2004). Antagonistic interaction

between abscisic acid and jasmonate-ethylene signaling pathways modulates defense gene expression and disease resistance in *Arabidopsis*. *The Plant Cell, 16*(12), 3460–3479.

Addrah, M. E., Zhang, Y. Y., Zhang, J., Liu, L., Zhou, H. Y., Chen, W. D., & Zhao, J. (2019). Fungicide treatments to control seed-borne fungi of sunflower seeds. *Pathogens, 9*(1), 29.

Boukaew, S., Plubrukam, A., & Prasertsan, P. (2013). Effect of volatile substances from *Streptomyces philanthi* RM-1-138 on growth of rhizoctonia solani on rice leaf. *BioControl, 58*(4), 471–482.

Cameron, D. D., Neal, A. L., van Wees, S. C. M., & Ton, J. (2013). Mycorrhiza-induced resistance: More than the sum of its parts? *Trends in Plant Science, 18*(10), 539–545.

Coleman, J. J. (2016). The *Fusarium solani* species complex: Ubiquitous pathogens of agricultural importance. *Molecular Plant Pathology, 17*(2), 146–158.

Chen, L., Wang, X. H., Ma, Q. H., Bian, L. S., Liu, X., Xu, Y., Zhang, H. H., Shao, J. H., & Liu, Y. P. (2020). *Bacillus velezensis* CLA178-induced systemic resistance of rosa multiflora against crown gall disease. *Frontiers in Microbiology*. https://doi.org/10.3389/fmicb.2020.587667

Dimopoulou, A., Theologidis, I., Liebmann, B., Kalantidis, K., Vassilakos, N., & Skandalis, N. (2019). *Bacillus amyloliquefaciens* MBI600 differentially induces tomato defense signaling pathways depending on plant part and dose of application. *Scientific Reports, 9*, 19120.

Etesami, H., & Alikhani, H. A. (2016). Rhizosphere and endorhiza of oilseed rape (*Brassica napus* L.) plant harbor bacteria with multifaceted beneficial effects. *Biological Control, 94*, 11–24.

Etesami, H., & Maheshwari, D. K. (2018). Use of plant growth promoting rhizobacteria (PGPRs) with multiple plant growth promoting traits in stress agriculture: Action mechanisms and future prospects. *Ecotoxicology and Environmental Safety, 156*, 225–246.

Evenhuis, A., Verdam, B., Gerlagh, M., & Goossen-van de Geijn, H. M. (1995). Studies on major diseases of caraway (*Carum carvi*) in the Netherlands. *Industrial Crops and Products, 4*(1), 53–61.

Fan, W. H., & Dong, X. N. (2002). In vivo interaction between *NPR1* and transcription factor *TGA2* leads to salicylic acid-mediated gene activation in *Arabidopsis*. *The Plant Cell, 14*(6), 1377–1389.

Feng, N. X., Yu, J., Mo, C. H., Zhao, H. M., Li, Y. W., Wu, B. X., Cai, Q. Y., Li, H., Zhou, D. M., & Wong, M. H. (2018). Biodegradation of di-n-butyl phthalate (DBP) by a novel endophytes *Bacillus megaterium* strain YJB3. *Science of the Total Environment, 616*, 117–127.

Fravel, D. R. (2005). Commercialization and implementation of biocontrol. *Annual Review of Phytopathology, 43*, 337–359.

Gorash, A., Armoniene, R., & Kazan, K. (2021). Can effectoromics and loss-of-susceptibility be exploited for improving Fusarium head blight resistance in wheat? *Crop Journal, 9*, 1–16.

Hallmann, J., Quadt-Hallmann, A., Mahaffee, W. F., & Kloepper, J. W. (1997). Bacterial endophytes in agricultural crops. *Canadian Journal of Microbiology, 43*(10), 895–914.

Ivanova, P., Dzięgielewski, K., Drozd, M., Skorupska, M., Grabowska-Jadach, I., & Mariusz, P. (2021). Nanoparticles of chosen noble metals as reactive oxygen species scavengers. *Nanotechnology*. https://doi.org/10.1088/1361-6528/abc19f

Jiao, R., Munir, S., He, P. F., Yang, H. W., Wu, Y. X., Wang, J. W., He, P. B., Cai, Y. Z., Wang, G., & He, Y. Q. (2020). Biocontrol potential of the endophytes *Bacillus amyloliquefaciens* YN201732 against tobacco powdery mildew and its growth promotion. *Biological Control*. https://doi.org/10.1016/j.biocontrol.2019.104160

Kumar, S., Nei, M., Dudley, J., & Tamura, K. (2008). MEGA: A biologist-centric software for evolutionary analysis of DNA and protein sequences. *Briefings in Bioinformatics, 9*(4), 299–306.

Lin, C. W., Chang, H. B., & Huang, H. J. (2005). Zinc induces mitogen-activated protein kinase activation mediated by reactive oxygen species in rice roots. *Plant Physiology and Biochemistry, 43*(10–11), 963–968.

Lian, L. L., Xie, L. Y., Zheng, L. P., & Lin, Q. Y. (2011). Induction of systemic resistance in tobacco against Tobacco mosaic virus by *Bacillus* spp. *Biocontrol Science and Technology, 21*(3), 281–292.

Lopes, R., Tsui, S., Gonçalves, P. J. R. O., & de Queiroz, M. V. (2018). A look into a multifunctional toolbox: Endophytes *Bacillus* species provide broad and underexploited benefits for plants. *World Journal of Microbiology and Biotechnology, 34*(7), 94.

Luna-Bulbarela, A., Tinoco-Valencia, R., Corzo, G., Kazuma, K., Konno, K., Galindo, E., & Serrano-Carreón, L. (2018). Effects of bacillomycin D homologues produced by *Bacillus amyloliquefaciens* 83 on growth and viability of *Colletotrichum gloeosporioides* at different physiological stages. *Biological Control, 127*, 145–154.

Livak, K. J., & Schmittgen, T. D. (2001). Analysis of relative gene expression data using real-time quantitative PCR and the 2(-Delta Delta C(T)) Method. *Methods, 25*(4), 402–408.

Li, H. X., Xiao, Y., Cao, L. L., Yan, X., Li, C., Shi, H. Y., Wang, J. W., & Ye, Y. H. (2013). Cerebroside C increases tolerance to chilling injury and alters lipid composition in wheat roots. *PLoS ONE, 8*(9), e73380.

Nazari, M., & Smith, D. L. (2020). A PGPR-produced bacteriocin for sustainable agriculture: A review of Thuricin 17 characteristics and applications. *Frontiers in Plant Science*. https://doi.org/10.3389/fpls.2020.00916

Ors, M., Randoux, B., Siah, A., Couleaud, G., Maumene, C., Sahmer, K., Reignault, P., Halama, P., & Selim, S. (2019). A plant nutrient- and microbial protein-based resistance inducer elicits wheat cultivar-dependent resistance against *Zymoseptoria tritici*. *Phytopathology, 109*(12), 2033–2045.

Peng, M. (1992). Peroxidase-generated hydrogen peroxide as a source of antifungal activity in vitro and on Tobacco leaf disks. *Phytopathology, 82*(6), 696–699.

Rabiey, M., Hailey, L. E., Roy, S. R., Grenz, K., Al-Zadjali, M. A. S., Barrett, G. A., & Jackson, R. W. (2019). Endophytes vs tree pathogens and pests: Can they be used as

biological control agents to improve tree health? *European Journal of Plant Pathology, 155*(3), 711–729.

Ren, J. H., Li, H., Wang, Y. F., Ye, J. R., Yan, A. Q., & Wu, X. Q. (2013). Biocontrol potential of an endophytes *Bacillus pumilus* JK-SX001 against poplar canker. *Biological Control, 67*(3), 421–430.

Rooney, A. P., Price, N. P. J., Ehrhardt, C., Swezey, J. L., & Bannan, J. D. (2009). Phylogeny and molecular taxonomy of the *Bacillus subtilis* species complex and description of *Bacillus subtilis* subsp. inaquosorum subsp. nov. *International Journal of Systematic and Evolutionary Microbiology, 59*, 2429–2436.

Romero-Puertas, M. C., Rodriguez-Serrano, M., Corpas, F. J., Gomez, M., Del Rio, L. A., & Sandalio, L. M. (2004). Cadmium-induced subcellular accumulation of $O^{2\cdot-}$ and $H_2O_2$ in pea leaves. *Plant Cell and Environment, 27*(9), 1122–1134.

Sánchez Hernández, M. E., Ruiz Dávila, A., Pérez de Algaba, A., Blanco López, M. A., & Trapero Casas, A. (1998). Occurrence and etiology of death of young olive trees in southern Spain. *European Journal of Plant Pathology, 104*, 347–357.

Selim, S., Martin-Laurent, F., Rouard, N., Gianinazzi, S., & van Tuinen, D. (2007). Impact of a new biopesticide produced by *Paenibacillus* sp. strain B2 on the genetic structure and density of soil bacterial communities. *Pest Management Science, 63*(3), 269–275.

Srikhong, P., Lertmongkonthum, K., Sowanpreecha, R., & Rerngsamran, P. (2018). *Bacillus* sp. strain M10 as a potential biocontrol agent protecting chili pepper and tomato fruits from anthracnose disease caused by *Colletotrichum capsici*. *BioControl, 63*(6), 833–842.

Schmitt, F. J., Renger, G., Friedrich, T., Kreslavski, V. D., Zharmukhamedov, S. K., Los, D. A., Kuznetsov, V. V., & Allakhverdiev, S. I. (2014). Reactive oxygen species: Re-evaluation of generation, monitoring and role in stress-signaling in phototrophic organisms. *Biochimica Et Biophysica Acta Bioenergetics, 1837*(6), 835–848.

Tashi-Oshnoei, F., Harighi, B., & Abdollahzadeh, J. (2017). Isolation and identification of endophytes bacteria with plant growth promoting and biocontrol potential from oak trees. *Forest Pathology, 47*(5), e12360.

Van Loon, L. C. (2007). Plant responses to plant growth-promoting rhizobacteria. *European Journal of Plant Pathology, 119*, 243–254.

Wang, J. F., Zhang, Y. Q., Li, Y., Wang, X. M., Nan, W. B., Hu, Y. F., Zhang, H., Zhao, C. Z., Wang, F., Li, P., Shi, H. Y., & Bi, Y. R. (2015). Endophytes microbes *Bacillus* sp. LZR216-regulated root development is dependent on polar auxin transport in *Arabidopsis* seedlings. *Plant Cell Reports, 34*(6), 1075–1087.

Whipps, J. M. (1997). Developments in the biological control of soil-borne plant pathogens. *Advances in Botanical Research, 26*, 1–134.

Wu, L. M., Huang, Z. Y., Li, X., Ma, L. M., Gu, Q., Wu, H. J., Liu, J., Borriss, R., Wu, Z., & Gao, X. W. (2018). Stomatal closure and SA-, JA/ET-Signaling pathways are essential for *Bacillus amyloliquefaciens* FZB42 to restrict leaf disease caused by *Phytophthora nicotianae* in *Nicotiana benthamiana*. *Frontiers in Microbiology, 9*, 847.

Weiss, A., Delproposto, J., & Giroux, C. N. (2014). High-throughput phenotypic profiling of gene-environment interactions by quantitative growth curve analysis in *Saccharomyces cerevisiae*. *Analytical Biochemistry, 327*(1), 23–34.

Xie, S., Vallet, M., Sun, C., Kunert, M., David, A., Zhang, X. C., Chen, B. H., Lu, X. M., Boland, W., & Shao, Y. Q. (2020). Biocontrol potential of a novel endophytes bacterium from Mulberry (*Morus*) tree. *Frontiers in Bioengineering and Biotechnology, 7*, 488.

Yaish, M. W., Antony, I., & Glick, B. R. (2015). Isolation and characterization of endophytes plant growth-promoting bacteria from date palm tree (*Phoenix dactylifera* L.) and their potential role in salinity tolerance. *Antonie Van Leeuwenhoek International Journal of General and Molecular Microbiology, 107*(6), 1519–1532.

Yang, X. J., Chen, F. R., Gan, L., Du, Y. X., & Ruan, H. C. (2010). Effect of the endophytes *Bacillus subtilis* EBT1 isolated from banana on the growth and resistance to *Fusarium* wilt disease in banana. *Acta Phytophylacica Sinica, 37*(4), 300–306.

Yang, F., Li, W. S., Derbyshire, M., Larsen, M. R., Rudd, J. J., & Palmisano, G. (2015). Unraveling incompatibility between wheat and the fungal pathogen *Zymoseptoria tritici* through apoplastic proteomics. *BMC Genomics, 16*, 362.

Yamamoto, S., & Harayama, S. (1995). PCR amplification and direct sequencing of *gyrB* genes with universal primers and their application to the detection and taxonomic analysis of pseudomonas putida strains. *Applied and Environmental Microbiology, 61*(10), 3768.

Yanez-Mendizabal, V., Zeriouh, H., Vinas, I., Torres, R., Usall, J., de Vicente, A., Perez-Garcia, A., & Teixido, N. (2012). Biological control of peach brown rot (*Monilinia* spp.) by *Bacillus subtilis* CPA-8 is based on production of fengycin-like lipopeptides. *European Journal of Plant Pathology, 132*(4), 609–619.

Zhang, C. X., Zhang, X. X., & Shen, S. H. (2014). Proteome analysis for antifungal effects of *Bacillus subtilis* KB-1122 on *Magnaporthe grisea* P131. *World Journal of Microbiology and Biotechnology, 30*(6), 1763–1774.